

## Chapter 2

# Experimental techniques for surface physics

### 2.1 Photoemission spectroscopy

Photoemission spectroscopy is one of the most popular techniques for surface investigations. It is based on the photoelectric effect where the emission of electrons from a material is due to photon irradiation [8], and explained exactly 100 years ago by Einstein. In a photoemission experiment, a collimated beam of monochromatic photons of energy  $\hbar\omega$  is directed towards a sample. Electrons are then optically excited from occupied to unoccupied states in the solid and some of them leave the sample if  $\hbar\omega$  is larger than the sample work function  $\Phi$  and if their momentum is directed towards the surface.

Their kinetic energy distribution, which reflects their binding energy distribution in the solid, is then analysed. A photoemission experiment can be carried out under various conditions depending on the photon energy range and characteristics of the electron analyser. One can separate, in this way, the study of valence bands and core level lines and can obtain information from electrons with either a well defined escaping angle or in an angle integrated mode. In the former case, it is possible to study the electronic valence band dispersion with wave vector or to vary the depth of escaping electrons by changing the emission angle. The two major classes of photoemission experiments are valence and core level spectroscopy. In the first case low energy photons ( $10^1\text{eV}$ -  $10^2\text{eV}$ ) are generally used, while in the second class

of experiments a higher photon energy is required ( $10^2\text{eV}$ - $10^4\text{eV}$ ).<sup>1</sup>

Photoemission is a many-body process involving electron-photon, electron-electron and electron-phonon interactions. Its full quantum-mechanical description, known as the one-step model, takes all these effects into account [9].

In this approach the photocurrent (or the transition probability per unit time) can be described in terms of the Fermi's golden rule [10]:

$$j(\mathbf{R}, E, \hbar\omega) \propto \sum_{ioccup} |\langle \Phi_{<}^* | \delta H | \Phi_i \rangle|^2 \delta(E_i - \hbar\omega - E_f) \quad (2.1)$$

where the final state is taken as a time-reversed LEED wave  $\Phi_{<}^*$ ,  $\Phi_i$  represents the initial state, *ioccup* are the occupied states, and  $\delta H$ , the perturbation, is the dipole operator of the optical transition, given by the vector potential  $\mathbf{A}$  of the field and the electron momentum operator  $\mathbf{p} = -i\hbar\nabla$  as:

$$\delta H \propto \mathbf{A} \cdot \mathbf{p} + \mathbf{p} \cdot \mathbf{A}. \quad (2.2)$$

The matrix element  $M_{fi} \propto |\langle \Phi_{<}^* | \delta H | \Phi_i \rangle|^2$  describes all aspects of the photoemission process (optical excitation, transport through the solid and escape through the surface). One-step theories imply wave function matching at the surface, and allow the treatment of the whole set of situations encountered in photoemission: bulk and surface photoemission, adsorbates, etc.

A simpler and more instructive description, the semi-classical three-step model, accounts for many of the features observed experimentally. In this model, the photoemission process is regarded as separated into three consecutive events: optical excitation, transport to the surface and escape through the surface potential barrier [9]. In the first step, a photon with energy  $\hbar\omega$  is absorbed and an electron is excited from an occupied to an unoccupied state within the crystal. The momentum carried by a photon is small and, therefore, the crystal momentum  $\hbar\mathbf{k}$  is conserved via the exchange of a reciprocal lattice momentum vector  $\hbar\mathbf{G}$  between the electron and the periodic lattice. The momentum conservation rule can thus be written:

$$\mathbf{k}_f = \mathbf{k}_i + \mathbf{G} \quad (2.3)$$

---

<sup>1</sup>Of course this distinction is not as abrupt as it may appear. For example, it is worth to remember that valence band studies can be done at very high energies, using the resonant phenomena of valence photoemission and Auger decay. Anyway, in the use of photoemission that we have done to study our systems, this distinction is still well defined.

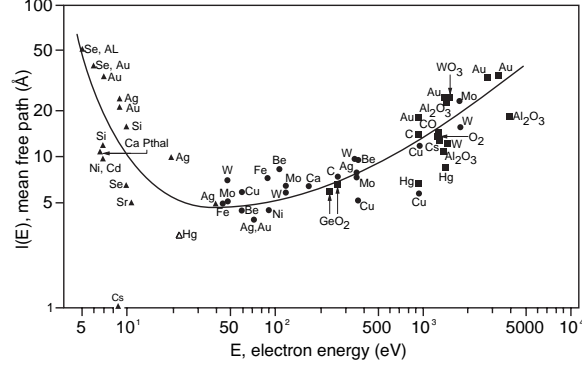


Figure 2.1: Escape depth versus kinetic energy of the electron measured for different materials. After ref. [11].

while energy conservation imposes the condition:

$$E(\mathbf{k}_f) = E(\mathbf{k}_i) + \hbar\omega, \quad (2.4)$$

where  $\mathbf{k}_f$  and  $\mathbf{k}_i$  mean, respectively, the final and initial momentum. Thus, the transition is vertical and can take place only at positions where the energy difference between initial and final energy equals  $\hbar\omega$ .

In the second step, the excited electron propagates through the crystal and eventually reaches the surface. Strong electron-electron interaction may result in scattering events in which both energy and direction of the traveling electron is changed. The probability for such a scattering event to occur is described by a parameter  $\lambda$  called the “electron mean free path”, which represents the average distance a photoelectron travels between two inelastic scattering events, and determines the electron escape depth. The electron escape depth is dependent on the kinetic energy and, while it depends weakly on the actual material, has generally a minimum of about 5 Å at a kinetic energy of about 50 eV (see figure 2.1).

The third step, in which the photoelectron escapes through the surface, is characterized by the conservation of the electron surface-parallel wave vector component  $\mathbf{k}_{f\parallel}$  to within a surface reciprocal lattice vector  $\mathbf{g}_{\parallel}$

$$\mathbf{q}_{\parallel} = \mathbf{k}_{f\parallel} + \mathbf{g}_{\parallel} \quad (2.5)$$

where  $\mathbf{q}_{\parallel}$  and  $\mathbf{k}_{f\parallel}$  are the external and internal surface-parallel wave vector

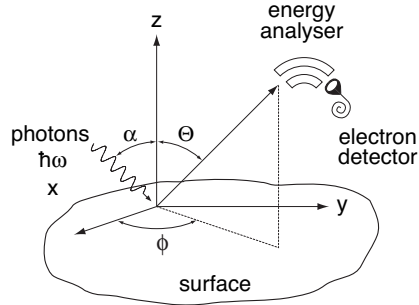


Figure 2.2: Schematic representation of the angle resolved photoemission geometry.

components of the photoelectron, respectively. For an unreconstructed surface,  $\mathbf{g}_{\parallel}$  is the surface-parallel component of a reciprocal bulk lattice vector  $\mathbf{G}$ .

### 2.1.1 Angle resolved spectroscopy

The principle and geometry for angle-resolved ultraviolet photoelectron spectroscopy or ARUPS is shown schematically in Fig. 2.2. The angle resolved analyzer collects electrons escaping from the surface with an angle  $\Theta$ . Since the translational symmetry of the crystal potential is broken in the direction normal to the surface, the wave vector component  $k_{\perp}$  perpendicular to the surface is not conserved as the electron escapes into the vacuum, but, as indicated before, the parallel components are conserved. Thanks to conservation of wave vector and energy for a photoelectron escaping without scattering, its kinetic energy and propagation direction in vacuum gives information about the initial state from which it was excited. Since an electron in vacuum is free, for an emitted photoelectron the following dispersion relation holds:

$$E_{kin} = E(\mathbf{k}_{\mathbf{f}}) - E_V = \frac{\hbar^2 q^2}{2m} \quad (2.6)$$

where  $E_V$  is the vacuum potential. Combination of the above relation with equations 2.3 and 2.5 gives the surface parallel component of the wave vector in the initial state as

$$\mathbf{k}_{i\parallel} = \sqrt{\frac{2mE_{kin}}{\hbar^2}} \sin \Theta \frac{\mathbf{q}_{\parallel}}{|\mathbf{q}_{\parallel}|} - \mathbf{G}_{\parallel} - \mathbf{g}_{\parallel}. \quad (2.7)$$

Furthermore, using equations 2.3 and 2.6 together with the definition of the work function  $\Phi = E_V - E_f$ , we obtain the initial state energy as:

$$E(\mathbf{k}_i) - E_F = E_{kin} + \phi - \hbar\omega \quad (2.8)$$

where  $E_F$  is the Fermi energy. Thus by knowing  $E_{kin}$ ,  $\Theta$  and  $\Phi$ , the parallel wave vector component  $\mathbf{k}_{i\parallel}$  and energy  $E(\mathbf{k}_i)$  of the initial state are easily calculated. Since  $k_{f\perp}$  is not conserved upon transmission through the surface, the perpendicular wave vector component  $k_{i\perp}$  cannot be directly obtained from an ARUPS measurement. However, the final state band is in many cases reasonably well described by a free-electron parabola with a constant inner potential,  $V_0$ :

$$E(\mathbf{k}_f) = \frac{\hbar^2}{2m}(k_{f\parallel}^2 + k_{f\perp}^2) \quad (2.9)$$

with

$$k_{f\perp}^2 = q_{\perp}^2 + \frac{2mV_0}{\hbar^2} \quad (2.10)$$

where  $\mathbf{q}$  is the photoelectron wave vector outside the sample (the measured one). From this condition,  $k_{i\perp}$  can be estimated using equations 2.3 and 2.5. Hence, angle resolved photoemission gives the possibility to study the bulk and surface band dispersion by varying the angle at which the electrons are detected by the analyzer, obtaining  $E(\mathbf{k})$ .

### 2.1.2 Core level spectroscopy

The number of core levels and their binding energies are characteristic for a given chemical element. These parameters can therefore be utilized for an elemental analysis of the material being used. Moreover, the actual core level binding energy of an element in a solid is given by the chemical environment in which it lies. A comprehensive investigation of the core level line shape, thus, gives detailed information about the chemical environment of the atom studied [12]. The basic physics underlying the change in binding energy is simple. The energy of an electron in a tightly bound core state is determined by the attractive potential of the nuclei and the repulsive core Coulomb interaction with all the other electrons. A change in the chemical environment of a particular atom involves a spatial rearrangement of the valence charges of this particular atom and a different potential created by the nuclear and electronic charges on all the other atoms in the compound.

This simple picture is reflected in a similarly simple relationship connecting the binding energy difference  $\Delta E_i^c(A,B)$  of a core level  $c$  measured for an atom  $i$  in two different compounds A and B and the valence charges  $q^A$  and  $q^B$ , respectively,

$$\Delta E_i^c(A, B) = K_c(q^A - q^B) + (V_i^A - V_i^B). \quad (2.11)$$

The first term accounts for the charge transfer and the consequent difference in the electron-electron interaction between the core orbital and this valence charge.

The second term has the character of a Madelung potential. This term decreases the observed shift  $E_i$  so that shifts are usually only a few eV or less [4]. Particularly spectacular is the case when A is an elemental material and B a compound of A and a ligand. Figure 2.3 shows two of such cases where core level shifts are directly related to differences in electronegativity between Si and the ligand. However, it has to be pointed out that the system has to rearrange also because of the principal effect of photoemission: the ionization of the atom involved. This rearrangement involves a flow of negative charge towards the hole created in the photoemission process in order to screen the suddenly appearing positive charge. The screening lowers the energy of the hole state left behind and therefore lowers the measured binding energy as well. This binding energy defect is commonly referred to as the relaxation energy  $E_R$  [9].

Thus, in core level photoemission, core level electrons are excited by photons and collected by the electron analyser. The typical energy resolution in an ESCA experiment is of the order of 100 meV, depending on the energy resolution of both the light source and the analyser, i.e. of the same order of the core level shifts. An accurate analysis of the core level shifts needs, therefore, a fitting procedure to decompose the core level line shape into various components corresponding to atoms in different chemical environment. The line shape of the core level for non-metallic samples can be described to a reasonable approximation by a Voigt function, which approximates a convolution of a Gaussian and a Lorentzian line shape. The Lorentzian curve accounts for the finite lifetime of the electron-hole pair, while the Gaussian curve is related to experimental broadening and surface disorder [12]. The Lorentzian distribution, with a width  $\Gamma_{FWHM}$ , which can be called the intrinsic width of a line, and is related to the lifetime  $\tau$  of the hole left behind the photoemission process through Heisenberg's uncertainty

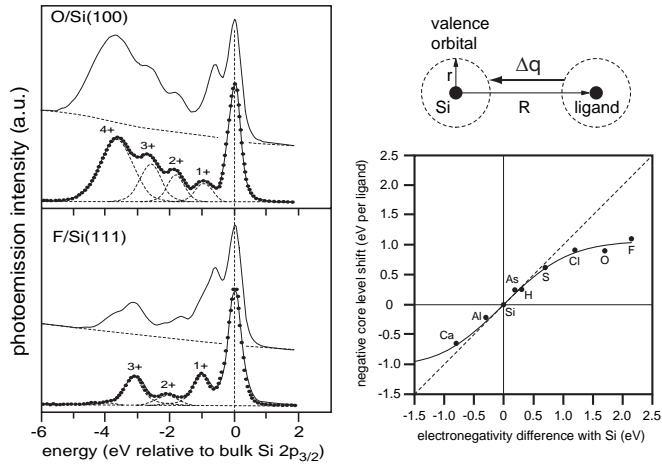


Figure 2.3: Photoemission spectra of the systems O/Si(001) and F/Si(111). Atoms in different environment (in this case with different ligancy) contribute with peaks of different shift (left). This is related more generally to the different electronegativity of Si and the ligand (right) [From Himpsel *et al.*, NATO Varenna Summer School 1988, Ed. Compagna and Rosei, North-Holland Publ.].

relation  $\Gamma = \tau^{-1}$ , has the character of a transition probability: a state with a core hole decays through a transition into a state of lower energy. Depending on the decay channels available to the core hole, it is possible to infer the dependence of the Lorentzian width on the core level excited: a  $1s$  core hole in a heavy atom will generally have a shorter life-time and will therefore be broader than a higher lying  $4f$  state because more levels are available to fill the deep-lying  $1s$  hole.

## 2.2 LEED and STM

As a complement to photoemission spectroscopy, in our work other two surface techniques have been used, i.e low energy electron diffraction (LEED) and scanning tunneling microscopy (STM).

The *Scanning Tunneling Microscope* (STM) is based on the quantum mechanical tunneling effect, in which electrons from one conductor may penetrate into another one passing through (“tunneling”) a potential barrier. The tunneling is granted by the leaking of the wave function of a surface

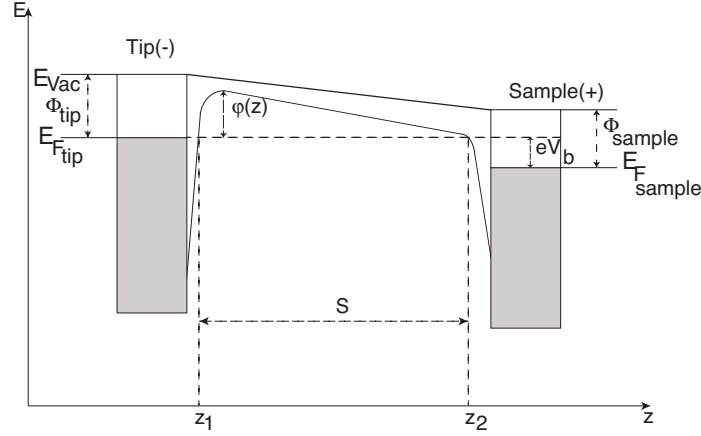


Figure 2.4: Representation of a tunnel contact in STM. A positive bias is applied to the sample. The form of the potential  $\varphi(z)$  is rounded by the image potential.

electron into the vacuum. The tunneling probability  $T$  depends on the distance  $d$  between the two conductors (the wave function decays exponentially into the vacuum) and on the barrier height  $\phi$ , the work function, as follows:

$$T(E) \approx \exp\left[-\frac{2d}{\hbar} \sqrt{2m(\phi - E)}\right]. \quad (2.12)$$

For an arbitrary potential  $\varphi(z)$  the WKB quasi-classical approximation (when the potential varies slowly with respect to the electron wavelength) is given by the equation:

$$T(E) = \exp\left[-\frac{2}{\hbar} \int_{z_1}^{z_2} \sqrt{2m[\varphi(z) - E]} dz\right]. \quad (2.13)$$

In a STM experiment, the sample is held at a biased potential ( $V_b$ ) to shift the Fermi edge of the sample with respect to the tip. In this way the barrier height and the spatial shape can be adjusted to produce a tunnel current  $I$ . A typical experimental situation is depicted in Fig. 2.4, in which a positive bias is applied, making possible the tunneling from the tip to unoccupied states in the sample. An STM image is obtained by maintaining either the current or the distance constant, and recording the variation of the free parameter to define the contour of the sample surface. In this way, the tip is moved in the lateral direction to scan a large region of the sample and the contour of this surface region is displayed.



The analysis of *low energy electron diffraction* (**LEED**) patterns from surfaces of solids is a well established technique for the investigation of surface periodicity. Electrons of kinetic energies in the range of 10 eV to 300 eV have de Broglie wavelengths comparable to interatomic distances. Illuminating a surface with a mono-energetic beam of such electrons will give rise to a well defined diffraction pattern of the elastically scattered electrons. As a result of the short mean free path of electrons in this energy region, this scattering only probes the surface layers. If only the top layer is involved in the scattering process, it can be shown that the diffraction spots appear when the parallel components of the wave vectors of incoming and outgoing electron waves fulfill the condition

$$\mathbf{k}_{\parallel}^{\text{out}} - \mathbf{k}_{\parallel}^{\text{in}} = \mathbf{G}_{2D} \quad (2.14)$$

where  $\mathbf{G}_{2D}$  is a reciprocal surface-lattice vector. That is, periodic structures on the sample lead to constructive interference of the backscattered electrons and the diffraction pattern is therefore a representation of the reciprocal lattice vectors of the surface. Experimentally, a filament emits electrons which are accelerated by a variable voltage and focused on the sample surface with deflection electrodes. The diffracted electrons are retarded between a set of grids in front of a fluorescent screen, in order to discriminate inelastically scattered electrons. Finally, the electrons passing the grids are accelerated onto the fluorescent screen, where they are converted into visible intensity variations.

## 2.3 Ultra high vacuum

The short mean free path of the photoelectrons makes the preparation and preservation of a clean sample surface one of the main experimental tasks in photoemission. For example, at an escape depth of 10 Å, assuming a lattice constant of 4 Å, and an exponential decay of the photoemission intensity with depth, we find that the topmost layer of atoms contributes about 30% to the total spectrum. It is therefore clear that even partial changes in the topmost layer that are not intrinsic to the material under study (surface reconstruction, for example) can severely falsify the results. A foreign atom on the surface may add its own photoemission lines to the spectrum of the substrate; for example, oxygen contamination results in the addition of the

O  $1s$  line at 534 eV in core level spectroscopy or the O  $2p$  line around 6 eV binding energy and is therefore observable in the valence band spectra.

However, the interaction between adatom and substrate may change the energy levels of the substrate as well and induce a substrate core level shift. The conservation of a clean sample requires, therefore, ultrahigh vacuum conditions (UHV). In fact, a sample exposed to a gas at a pressure of  $10^{-6}$  Torr that has a sticking coefficient of unity will accumulate a monolayer of that gas in 1 s. The sticking probability can vary by several orders of magnitude depending on the material. The (111) surface of nickel, for example, has a sticking probability probability of 1 for CO, making the operation at pressures as low as  $10^{-10}$ – $10^{-11}$  Torr necessary in order to have sufficient time for an experiment.